N.A.E.

R. & M. No. 2795
(13,896)
A.R.C. Technical Report

MINISTRY OF SUPPLY

AERONAUTICAL RESEARCH COUNCIL
REPORTS AND MEMORANDA

Theoretical Supersonic Drag of Non-lifting Infinite-span Wings Swept behind the Mach Lines

By

T. NONWEILER, B.Sc.

LONDON: HER MAJESTY'S STATIONERY OFFICE
1954
SIX SHILLINGS NET

Theoretical Supersonic Drag of Non-lifting Infinite-span Wings Swept behind the Mach Lines

By

T. NONWEILER, B.Sc.

COMMUNICATED BY THE PRINCIPAL DIRECTOR OF SCIENTIFIC RESEARCH (AIR), MINISTRY OF SUPPLY

*Reports and Memoranda No. 2795**

October, 1950

Summary.—The drag of a non-lifting swept wing of infinite span is investigated for supersonic flow when the Mach lines from the wing apex lie ahead of the wing leading-edge. The wing section is assumed to be arbitrary but identical over the entire wing-span. The drag is found according to the linear equations of supersonic flow by considering the flow due to a system of superposed source planes.

The drag of such a wing is found to be finite and the effect of the speed of flight independent of the section shape assumed. The variation of drag with the section shape is shown to be proportional to the integral over the chord of the product of the local wing thickness and the value of the excess pressure existing in incompressible flow at the same position. The drag of wing-sections given by certain types of formula is evaluated in general terms, and some numerical results are given: the drag of sections with bluff noses and finite trailing-edge angles is generally between 0 and 15 per cent greater than the drag of a wing of the same sweep and thickness having a biconvex section.

Finally, methods of reducing the drag by changing the section shape are considered.

1. *Introduction.*—A question which is often raised in connection with supersonic aircraft is: how does the section shape affect the drag of a swept wing? Experimental information on this point is at present limited, and the existing theoretical work is largely confined to wings of biconvex or double-wedge section: it is possible to determine the theoretical wave drag of other sections, but with the more 'realistic' types of section shape the expressions to be evaluated are so lengthy that the amassing of a comprehensive set of results presents a formidable programme of computation[6]. Not only would such an analysis have to deal with the effect of section shape, but also with the variation of drag with aspect ratio and taper ratio, as well as with flight speed.

We shall here try to isolate the effect of section shape, by dealing only with constant-chord wings of infinite span having the same section at all spanwise positions. Clearly there is then no variation of aspect ratio or taper ratio to be considered; nor, as we shall see, does the effect of flight speed modify the relative drag of various sections. We assume that the speed of flight is

* R.A.E. Tech. Note Aero. 2073, received 3rd April, 1951.

sufficiently low that the Mach lines from the wing apex lie ahead of the wing leading edge; this is the only case of interest at the present time—indeed, if this condition is not satisfied the question we have posed is a trivial one.

It might seem that results for an infinite wing would, even so, be of little application. Certainly the results obtained do not apply exactly to finite wings but there is good reason to suppose that they will afford a guide to the general problem as the drag of a finite constant-chord swept wing is concentrated in the region of the root, and above a certain aspect ratio, increases in the span cause little or no increase in wave drag, as will be shown below.

Again, it may be objected that the effects of taper ratio are important; this is certainly so, but a comparison of the relative drag of tapered wings of various sections would obviously depend upon the choice of a representative line of sweepback. No general conclusions on the effect of section shape alone can be drawn if the effect of varying sweepback is also included. This problem is outside the scope of the present investigations.

We shall deal with sections, amongst others, which have round noses and for this reason we have to find the drag on a streamtube rear the wing surface and then to find the drag of the wing by allowing this streamtube to approach the surface. This method is necessary as R. T. Jones has shown[5] that in the type of 'subsonic' flow existing over the wing far outspan there is a contribution to the drag associated with the singularity at the round nose which is not included if we merely intergrate the pressure over the wing surface.

From the general theory for the drag of an infinite wing we shall consider three applications:—

(a) We shall state the results in several forms which are of particular use when the wing section is defined by certain types of formula, or its subsonic pressure distribution is known.

(b) We shall work out a few numerical examples to show the relative drags of various types of well-known sections.

(c) We shall seek to find what features of the wing geometry are of importance both from the aspect of contributing to the drag and of reducing it.

2. *Drag of an Infinite Swept Wing.*—According to the three-dimensional linear theory of supersonic flow[1], a uniform plane distribution of sources in the plane $z = 0$, bounded upstream by the line $y = m(x - \xi)$ and by the x-axis will produce, if

$$m\sqrt{(M^2 - 1)} = \mu \leqslant 1$$

i.e., if the Mach lines, from $x = \xi$, are ahead of the plane source, a pressure distribution given by*

$$\frac{\Delta p}{q} = \frac{2}{\pi}\,\varepsilon\,\frac{m}{\sqrt{(1-\mu^2)}}\,\mathscr{R}\left\{\operatorname{arg\,cosh}\left[\frac{X - \xi + (1-\mu^2)\dfrac{y}{m}}{\mu\sqrt{\left((X-\xi)^2 + (1-\mu^2)\dfrac{z^2}{m^2}\right)}}\right]\right\} \quad \ldots \quad (1)$$

where $X = x - \dfrac{y}{m}$, and ε is a constant.

---

* Here 'arg cosh' denotes the inverse hyperbolic cosine, as in American papers; later the function 'ln' is introduced to denote natural logarithms.

The distribution of velocity in the z-direction is given by

$$\frac{w}{U} = -\frac{\partial}{\partial z}\int_{-\infty}^{x} \frac{1}{2}\left(\frac{\Delta p}{q}\right) dx \quad \ldots \quad (2)$$

and it may be shown that as $z \to 0$,

$$\left.\begin{aligned} \frac{w}{U} &= \operatorname{sgn}(z)\ \varepsilon \qquad \text{for } y \geqslant 0, \quad X > \xi \\ &= 0 \qquad \text{for } y \geqslant 0, \quad X < \xi, \text{ and for } y \leqslant 0 \end{aligned}\right\} \quad \ldots \quad (3)$$

Thus, for small values of ε this discontinuity in normal velocity satisfies the boundary condition for a semi-infinite oblique wedge having a small wedge angle 2ε, as shown in Fig. 1.

Similarly, by superposition, it may be shown that a uniform plane distribution of sources in the plane $z = 0$ bounded upstream by the lines $y = \pm m(x - \xi)$ will produce, if $\mu \leqslant 1$, a pressure distribution given by

$$\frac{\Delta p}{q} = \varepsilon[f(x - \xi, y, z) + f(x - \xi, -y, z)]$$

i.e.,

$$\frac{\Delta p}{q} = 2\varepsilon g(x - \xi, y, z), \text{ say} \quad \ldots \quad (4)$$

where, from (1),

$$f(x - \xi, y, z) = \frac{2}{\pi}\frac{m}{\sqrt{(1 - \mu^2)}}\ \mathcal{R}\left\{\operatorname{arg\,cosh}\left[\frac{x - \xi - \mu^2 \dfrac{y}{m}}{\mu\sqrt{\left[\left(x - \xi - \dfrac{y}{m}\right)^2 + (1 - \mu^2)\dfrac{z^2}{m^2}\right]}}\right]\right\}$$

and which satisfies the boundary condition for an infinite oblique wedge symmetrical about the x-axis and having a small wedge angle 2ε.

For the purposes of the present investigation we shall define such infinite source planes by their leading boundaries, and we shall call the quantity ε the strength of the source plane. Thus a system of such source planes formed by:—

(*a*) a source plane bounded by $y = \pm\, mx$ of strength $z'(0)$,

(*b*) a distribution of source planes bounded by $y = \pm\, m(x - \xi)$ of infinitesimal strength $z''(\xi)\, d\xi$, for all values of ξ where $0 \leqslant \xi < c$,

(*c*) a source plane bounded by $y = \pm\, m(x - c)$ of strength $-z'(c)$,

will together yield a flow which satisfies the boundary condition for an infinite swept wing with leading edges along $y = \pm\, mx$, trailing edges along $y = \pm\, m(x - c)$, and a thickness distribution $z = \pm\, z(X)$ as shown in Fig. 2.

The normal velocity distribution at any point due to the system of sources described above is given by

$$\frac{w}{U} = -\frac{\partial}{\partial z}\left[z'(0)\int_{-\infty}^{x} g(x, y, z)\, dx - z'(c)\int_{-\infty}^{x} g(x - c, y, z)\, dx\right.$$

$$\left. + \int_{0}^{c} z''(\xi)\left(\int_{-\infty}^{x} g(x - \xi, y, z)\, dx\right) d\xi\right]$$

$$= \frac{\partial}{\partial z}\left[\int_{0}^{c} z'(\xi)\frac{\partial}{\partial \xi}\left(\int_{-\infty}^{x} g(x - \xi, y, z)\, dx\right) d\xi\right]$$

and since $g = 0$ in front of the Mach cone from the point $x = \xi, y = 0$,

$$\frac{w}{U} = -\int_{0}^{c} z'(\xi)\frac{\partial g}{\partial z}\, d\xi\,. \qquad (5)$$

Similarly, the pressure distribution is given by

$$\frac{\Delta p}{q} = 2\int_{0}^{c} z'(\xi)\frac{\partial g}{\partial x}\, d\xi\,. \qquad (6)$$

Here the pressure field is described as due to a superposition of source lines each giving an incremental normal displacement $z'(\xi)\, d\xi$. This form of description is preferable to that of superposed source planes if $z'(0)$ is infinite.

Consider an infinite streamtube enclosing the wing whose section far upstream in the plane $x =$ constant is formed of the two straight lines $z = \pm\psi$.

The equation for a section of this streamtube in the plane $y =$ constant is, according to the linear theory, given by

$$\frac{dz}{dx} = \left.\frac{w}{U}\right|_{y} \qquad (7)$$

so that the drag on such a section is

$$q\int_{-\infty}^{+\infty}\frac{dz}{dx}\frac{\Delta p}{q}\, dx = -2q\int_{-\infty}^{+\infty}\left(\int_{0}^{c} z'(\xi)\frac{\partial g}{\partial z}\, d\xi\right)\left(\int_{0}^{c} z'(\xi)\frac{\partial g}{\partial x}\, d\xi\right) dx$$

where y is treated as a constant and z is related to x by equation (7). The drag on the complete wing is then given by

$$D = -8q\lim_{\psi\to 0}\int_{0}^{\infty} dy\int_{-\infty}^{+\infty}\left(\int_{0}^{c} z'(\xi)\frac{\partial g}{\partial z}\, d\xi\right)\left(\int_{0}^{c} z'(\xi)\frac{\partial g}{\partial x}\, d\xi\right) dx \qquad (8)$$

where the limit is taken to mean the value of the integrand as the streamtube selected approaches the surface.

From (4), if $x - \xi \geqslant \frac{\mu}{m}\sqrt{(y^2 + z^2)}$

$$\frac{\partial g}{\partial z} = -\frac{1}{\pi}\left[\left\{\frac{x - \xi - \mu^2 \frac{y}{m}}{\left(x - \xi - \frac{y}{m}\right)^2 + (1 - \mu^2)\frac{z^2}{m^2}} + \frac{x - \xi + \mu^2 \frac{y}{m}}{\left(x - \xi + \frac{y}{m}\right)^2 + (1 - \mu^2)\frac{z^2}{m^2}}\right\} \times \frac{\frac{z}{m}}{\sqrt{\left[(x - \xi)^2 - \mu^2\left(\frac{y^2}{m^2} + \frac{z^2}{m^2}\right)\right]}}\right]$$

$$\frac{\partial g}{\partial x} = \frac{1}{\pi}\left[\left\{\frac{\left(\frac{y^2}{m^2} + \frac{z^2}{m^2}\right) - \frac{y}{m}(x - \xi)}{\left(x - \xi - \frac{y}{m}\right)^2 + (1 - \mu^2)\frac{z^2}{m^2}} + \frac{\left(\frac{y^2}{m^2} + \frac{z^2}{m^2}\right) + \frac{y}{m}(x - \xi)}{\left(x - \xi + \frac{y}{m}\right)^2 + (1 - \mu^2)\frac{z^2}{m^2}}\right\} \times \frac{m}{\sqrt{\left[(x - \xi)^2 - \mu^2\left(\frac{y^2}{m^2} + \frac{z^2}{m^2}\right)\right]}}\right]$$

and both derivatives are zero if $x - \xi < \frac{\mu}{m}\sqrt{(y^2 + z^2)}$.

As was shown in Ref. 1, the integral

$$\int_0^c z'(\xi)\frac{\partial g}{\partial z}\,d\xi$$

vanishes as $z \to 0$, except for those values of x and y such that for some value of ξ between 0 and c,

$$x - \xi - \frac{y}{m} = 0$$

i.e., on or near the wing surface. Near such a point,

$$\lim_{z \to 0}\frac{\partial g}{\partial z} \to \lim_{z \to 0}\left[-\frac{z}{\pi m}\frac{\sqrt{(1 - \mu^2)}}{\left(x - \xi - \frac{y}{m}\right)^2 + (1 - \mu^2)\frac{z^2}{m^2}}\right]$$

and the integration may be confined to values of ξ close to $\left(x - \frac{y}{m}\right)$.

Thus, near $z = 0$, we may write equation (5) as

$$\frac{w}{U} = \frac{1}{\pi}\frac{z}{m}\sqrt{(1-\mu^2)}\int_0^c \frac{z'(\xi)\,d\xi}{(x-\xi)^2+(1-\mu)^2\dfrac{z^2}{m^2}} \quad \ldots \quad (9)$$

so that introducing independent variables X and y, from (7), $\frac{w}{U}$ and z become independent of y; and instead of (8) we may write

$$D = 8q \lim_{\psi\to 0}\lim_{b\to\infty}\left\{\int_{-\infty}^{+\infty}\left[\int_0^c z'(\xi)\left(\int_0^b \frac{\partial g}{\partial x}\bigg|_X dy\right)d\xi\right]\frac{w}{U}\,dX\right\} \quad \ldots \quad (10)$$

But if $(1-\mu^2)\frac{y}{m} \geqslant \mu\sqrt{\left((X-\xi)^2+(1-\mu^2)\frac{z^2}{m^2}\right)} - (X-\xi)$

$$\int \frac{\partial g}{\partial x}\bigg|_X dy = \left\{ \frac{m^2(3-\mu^2)}{2\pi(1-\mu^2)^{3/2}}\operatorname{arg\,cosh}\left[\frac{X-\xi+(1-\mu^2)\dfrac{y}{m}}{\mu\sqrt{\left((X-\xi)^2+(1-\mu^2)\dfrac{z^2}{m^2}\right)}}\right]\right.$$

$$-\frac{m^2(X-\xi)}{\pi(1-\mu^2)\left[(X-\xi)^2+(1-\mu^2)\dfrac{z^2}{m^2}\right]}\sqrt{\left[\left(X-\xi+\frac{y}{m}\right)^2-\mu^2\left(\frac{y^2}{m^2}+\frac{z^2}{m^2}\right)\right]}$$

$$-\frac{m^2}{2\pi}\frac{\left[2(X-\xi)\alpha-(1+\mu^2)\dfrac{z^2}{m^2}+(X-\xi)^2\right]}{\sqrt{\left\{\mathscr{D}\left[4\alpha^2+4(X-\xi)\alpha+(1-\mu^2)\dfrac{z^2}{m^2}+(X-\xi)^2\right]\right\}}}\operatorname{arc\,tan}\left[A\left(\frac{y}{m}-\alpha\right)\right]$$

$$\left.+\frac{m^2}{2\pi}\frac{\left[2(X-\xi)\beta-(1+\mu^2)\dfrac{z^2}{m^2}+(X-\xi)^2\right]}{\sqrt{\left\{\mathscr{D}\left[4\beta^2+4(X-\xi)\beta+(1-\mu^2)\dfrac{z^2}{m^2}+(X-\xi)^2\right]\right\}}}\operatorname{arg\,tanh}\left[B\left(\frac{y}{m}-\beta\right)\right]\right\}$$

where

$$A = \left(\frac{\mathscr{D}}{\left[4\alpha^2+4(X-\xi)\alpha+(1-\mu^2)\dfrac{z^2}{m^2}+(X-\xi)^2\right]\left[(1-\mu^2)\dfrac{y^2}{m^2}+2(X-\xi)\dfrac{y}{m}+(X-\xi)^2-\mu^2\dfrac{z^2}{m^2}\right]}\right)^{1/2}$$

$$B = \left(\frac{\mathscr{D}}{\left[4\beta^2+4(X-\xi)\beta+(1-\mu^2)\dfrac{z^2}{m^2}+(X-\xi)^2\right]\left[(1-\mu^2)\dfrac{y^2}{m^2}+2(X-\xi)\dfrac{y}{m}+(X-\xi)^2-\mu^2\dfrac{z^2}{m^2}\right]}\right)^{1/2}$$

$$\alpha = \frac{(1-\mu^2)\dfrac{z^2}{m^2} - (X-\xi)^2}{(X-\xi)} \qquad \beta = -\frac{2(X-\xi)}{(1-\mu^2)}$$

and

$$\mathscr{D} = \left[(1-\mu^2)(X-\xi)^2 + (1+\mu^2)^2 \frac{z^2}{m^2} \right]$$

On the other hand, if

$$(1-\mu^2)\frac{y}{m} < \mu\sqrt{\left((X-\xi)^2 + (1-\mu^2)\frac{z^2}{m^2}\right)} - (X-\xi)$$

then

$$\int \frac{\partial g}{\partial x}\bigg|_X dy = 0.$$

Hence if $b \to \infty$ and $z \to 0$,

$$\int_0^b \frac{\partial g}{\partial x}\bigg|_X dy \to \left\{ \frac{m^2(3-\mu^2)}{2\pi(1-\mu^2)^{3/2}} \ln \frac{1}{\sqrt{\left((X-\xi)^2 + (1-\mu^2)\dfrac{z^2}{m^2}\right)}} \right.$$

$$\left. - \frac{mb}{\pi\sqrt{(1-\mu^2)}} \frac{(X-\xi)}{\left[(X-\xi)^2 + (1-\mu^2)\dfrac{z^2}{m^2}\right]} + c_1 + c_2 \operatorname{sgn}(X-\xi) + O\left(\frac{1}{b}\right) \right\}$$

where c_1 and c_2 are constants involving b, and z has been included only in those connections which affect the singularities of the integral in the limit as $z \to 0$.

Now,

$$\lim_{\psi \to 0} \int_{-\infty}^{+\infty} \left[\int_0^c z'(\xi)[c_1 + c_2 \operatorname{sgn}(X-\xi)]d\xi \right] \frac{w}{U} dX = 0$$

so that

$$\frac{D}{q} = \lim_{\psi \to 0} \int_{-\infty}^{+\infty} (V_1 - V_2)\, dX$$

where

$$V_1 = \frac{4mz}{\pi^2}\left(\frac{3-\mu^2}{1-\mu^2}\right)\left\{ \int_0^c z'(\xi) \ln \frac{1}{\sqrt{\left((X-\xi)^2 + (1-\mu^2)\dfrac{z^2}{m^2}\right)}}\, d\xi \right\}$$

$$\times \left\{ \int_0^c \frac{z'(\xi)\, d\xi}{(X-\xi)^2 + (1-\mu^2)\dfrac{z^2}{m^2}} \right\}$$

$$V_2 = \frac{8bz}{\pi^2}\left\{ \int_0^c \frac{z'(\xi)(X-\xi)\, d\xi}{(X-\xi)^2 + (1-\mu^2)\dfrac{z^2}{m^2}} \right\}\left\{ \int_0^c \frac{z'(\xi)\, d\xi}{(X-\xi)^2 + (1-\mu^2)\dfrac{z^2}{m^2}} \right\}.$$

The integral involving V_2 is merely proportional to the drag force on the given wing section in two-dimensional incompressible flow, and may be shown to be zero, Hence

$$\frac{D}{q} = \lim_{\psi \to 0} \int_{-\infty}^{+\infty} V_1 \, dX.$$

This integral may be simplified by finding the limiting value of the integrand as $z \to 0$, and then integrating with respect to X whence

$$\frac{D}{q} = \frac{4m^2}{\pi} \frac{3 - \mu^2}{(1 - \mu^2)^{3/2}} \int_0^c z'(X) \left[\int_0^c \frac{z(\xi)}{\xi - X} \, d\xi \right] dX,$$

an expression which we shall put in a more useful form by writing

$$\frac{X}{c} = s, \quad \frac{\xi}{c} = \sigma, \quad z(X) = \frac{t}{2} \zeta(s)$$

where t is the maximum thickness of the wing.

Then,
$$\frac{D}{qm^2t^2} = \frac{1}{\pi} \frac{3 - \mu^2}{(1 - \mu^2)^{3/2}} I \quad \ldots \quad (11)$$

where

$$I = \int_0^{+1} \int_0^{+1} \zeta'(s) \, \zeta'(\sigma) \ln \left| \frac{1}{\sigma - s} \right| ds \, d\sigma \quad \ldots \quad (12)$$

This equation applies to wings of infinite span.

A more detailed examination of equation (10) will show that for wings of finite span, far outboard the local drag is negative and tends to zero inversely as the cube of the span. The drag of a high aspect ratio wing is, therefore, equal to the drag of the infinite wing if we neglect terms of order $1/A^2$ and higher compared with unity, where A is the aspect ratio. In terms of the drag coefficient based on the wing area S the drag of a finite wing of high aspect ratio is given by

$$C_D = \frac{D}{qS} = \frac{(t/c)^2}{\tan \Lambda} \frac{1}{\pi} \frac{3 - \mu^2}{(1 - \mu^2)^{3/2}} \frac{I}{A \tan \Lambda} .$$

For a wing of biconvex section $I = 4$, and a comparison of this approximation with correct theoretical values for finite untapered wings of biconvex section is shown in Fig. 3.

3. *Applications of Result.*—3.1. *Drag of Some Elementary Wing Sections with Round, Angular and Cusped Edges.*—The quantity D/qm^2t^2 as obtained from equation (11) is the product of two terms, one depending only on the Mach number and sweepback angle (*i.e.*, on μ), and the other a function only of the section geometry ; we may write

$$\frac{D}{qm^2t^2} = h(\mu) \frac{I}{4}$$

where
$$h(\mu) = \frac{4}{\pi} \frac{3 - \mu^2}{(1 - \mu^2)^{3/2}}$$

is plotted in Fig. 4.

At a given Mach number, two infinite wings of the same sweepback and thickness have a drag which is proportional only to I : accordingly the drag of various elementary sections* can usefully be quoted in terms of I as in Table 1 or Fig. 5.

* In the sections which follow we shall use the term 'drag of sections . . .' where we should more correctly write 'drag of an infinite swept wing with sections . . .'.

It may legitimately be objected that the theory is not applicable to sections with round noses, because the perturbation velocities are not small in the region of the nose. In particular, at the wing-root leading-edge the pressure is infinite: but far outspan the pressure distribution resembles that in linearised two-dimensional incompressible flow. However the analysis in section 2 remains valid if we allow $z'(0)$ to approach infinity.

Fig. 5 displays the fact that sections having a continuous slope and round edges generally have a high drag. The drag may be reduced by sharpening the edges, and still further reduced by cusping. The relatively low drag of the double-wedge sections is also evident. Most of the theoretical data on finite wings have been obtained for biconvex and double-wedge sections. It will be seen from Fig. 5, that the drag of the 'conventional' section, which resembles those commonly used on aircraft, is just over 10 per cent greater than a biconvex section, and over 60 per cent greater than a double-wedge section.

3.2. *Drag of Wing Sections expressed as a Fourier Series.*—Wing profiles are commonly derived from formulae of the type

$$\zeta(s) = \sum_{1}^{2m+1} \beta_n \sin n\theta, \quad \text{where} \left(\frac{1 - \cos\theta}{2}\right) = s \qquad \ldots \quad \ldots \quad \ldots \quad \ldots \quad (13)$$

with some modification of the shape near the trailing edge. It may be shown that for sections given by equation (13)

$$I = \frac{\pi^2}{2} \sum_{1}^{2m+1} n\beta_n^{\,2}. \qquad \ldots \quad \ldots \quad \ldots \quad \ldots \quad \ldots \quad \ldots \quad \ldots \quad \ldots \quad (14)$$

From equations (13) and (14), or otherwise, it may be shown that the profile having the least drag for a given cross-sectional area is the ellipse. However, apparently there is no optimum shape of profile having the least drag for a given thickness. It is always possible to find a section which has a drag less than any given finite value, so that the minimum value of I is theoretically zero. Such 'low-drag' sections as are obtained in this limiting process are characterised by their thin (or cusped) edges and very marked regions of concavity.

In section 4.4 it will be shown that any modification to the shape of a double-wedge section (with maximum thickness at half-chord) to produce less drag, will introduce a region of concave curvature.

Thus, of the sections having no concave curvature, the double-wedge section has the smallest drag for a given thickness.

3.3. *Drag of Wing Sections in Terms of the Subsonic Pressure Distribution.*—An alternative form for I which is of interest is obtained as follows:

$$I = \int_0^1 \zeta'(\sigma)\left(\int_0^1 \zeta'(s) \ln\left|\frac{1}{s - \sigma}\right| ds\right) d\sigma = \int_0^1 \zeta(\sigma)\left(\int_0^1 \frac{\zeta'(s)}{\sigma - s}\, ds\right) d\sigma$$

i.e.,

$$I = -\pi\left(\frac{c}{t}\right) \int_0^1 \zeta(\sigma) \left[\frac{\Delta p}{q}\right]_{\text{inc}} d\sigma \qquad \ldots \quad \ldots \quad \ldots \quad \ldots \quad \ldots \quad \ldots \quad (15)$$

where $\left[\dfrac{\Delta p}{q}\right]_{\text{inc}}$ is the pressure distribution over the section in linearised two-dimensional incompressible flow. Generally, special wing-sections are designed for a given simple low-speed pressure distribution, and together with the tabulated list of ordinates, equation (15) can be a useful method for computing I numerically—especially if the formal expression of the surface shape is obscure.

This method was used to compute the drag of the RAE 100–104 series of aerofoil sections* and the results are given in Table 2. The drag of these wings is only 5–10 per cent higher than the biconvex section.

Because most practical 'low-drag' sections are designed to have a more or less uniform pressure distribution in incompressible flow (*i.e.*, with no high suctions), it follows from equation (15) that their relative drags are roughly proportional to the sectional area.

3.4. *Drag of a Thin Wing Section derived from Conformal Transformation of Circle.*—If W is the complex potential of an incompressible flow (with velocity U parallel to the x-axis at infinity) about a thin profile, let us consider the expression

$$\int_C \left(\frac{dW}{dY} - U\right) Y\,dY = \int_C (u - U - iw)(x + iz)(dx + i\,dz) \qquad \qquad (16)$$

where C is a closed contour, u and w are the velocity components parallel to the x- and z-axes, and $Y = x + iz$.

We wish to find I, where, from equation (15), since the profile is thin, we have

$$I = \frac{4\pi}{t^2}\int_0^c \left(\frac{u - U}{U}\right) z\,dx \qquad \qquad (17)$$

Now if the contour C is formed by the zero streamline (including the upper surface of the profile) between $x = R$ and $-R$, and the large semicircle Γ in the upper half-plane of radius R about the origin, then, from equation (16), using the fact that on a streamline $w\,dx = u\,dz$,

$$\int_0^c (U - u) z\,dx = U\int_0^c z\,dx + \mathscr{I}\left\{\int_\Gamma \left(\frac{dW}{dY} - U\right) Y\,dY\right\}$$

$$- \mathscr{I}\left\{\int_C \left(\frac{dW}{dY} - U\right)\right\} Y\,dY \qquad \qquad (18)$$

where, since the profile is thin, we have neglected terms of powers higher than 2 in w/U and z/c. Thus the problem of finding I is reduced to that of evaluating the integrals on the right-hand side of equation (18).

Let us assume that the profile is derived from a transformation of a circle in the (ξ, ζ)-plane, where

$$Y = f(H) = H + \frac{\alpha_1}{H} + \frac{\alpha_2}{H^2} + \ldots\ldots \qquad \qquad (19)$$

and where $H = \eta + i\zeta$. Now, in the absence of circulation, if the profile is symmetrical about the x-axis,

$$W = U\left(H' + \frac{a^2}{H'}\right) \qquad \qquad (20)$$

where $H' = H - h$, h being a positive constant $< a$, and a being the radius of the circle to be transformed.

* The sections were calculated to give a 'roof-top' pressure distribution by the linear incompressible-flow theory, and the section ordinates are given in Ref. 2.

It follows that in equation (18), if we let $R \to \infty$,

$$\int_0^c \frac{(u - U)}{U} z(x)\, dx = [\pi(a^2 - \alpha_1^*) - V] \qquad (21)$$

where

$$V = \int_0^c z(x)\, dx, \text{ and } \alpha_1^* = \mathscr{R}(\alpha_1).$$

Thus, from (17)

$$I = \frac{4\pi}{t^2} [\pi(a^2 - \alpha_1^*) - V]. \qquad (22)$$

Now from equation (12) it is clear that the value of I depends only on the profile, or relative shape, and is independent of the thickness/chord ratio of the section. But it is important that in (22) the values of t and V are those for which the values of a and α_1 obtain; *i.e.*, they are the geometrical characteristics of the profile obtained by the transformation.

As a simple example, consider the Joukowski transformation given by $\alpha_1 = ka^2$ and $\alpha_2 = \alpha_3 = \ldots = 0$. This transforms the circle with centre at the origin into an ellipse with a thickness/chord ratio of $(1 - k)/(1 + k)$. From equation (22) we find

$$I = \frac{\pi^2}{2}$$

as obtained in section 3.1.

3.5. *Drag of Wing Sections Given by General Algebraic Formulae.*—Generally, the expression for the shape of an aerofoil in terms of a Fourier series (as in equation (13)) is inadequate because the trailing edge is either cusped or round. For this reason, if a wing section is derived to give a certain pressure distribution and is expressed as a Fourier series the section shape is often modified over the rear part to give a finite trailing-edge angle, and to remove any concave curvature. Once this is done it is not possible to express the drag in such a simple manner as described in equation (14), and the elegance of this method of expression is lost.

Generally, it is possible to fit wing sections to a formula of the type* :—

$$\left.\begin{aligned} \zeta &= \zeta_1(s) \quad (0 \leqslant s \leqslant s_0) \\ \zeta &= \zeta_2(s) \quad (s_0 \leqslant s \leqslant 1) \end{aligned}\right\} \qquad (23)$$

where

$$\zeta_1(s) = \sum_{n=0}^{2m} a_n s^{n/2}$$

and

$$\zeta_2(s) = \sum_{n=0}^{2m} b_n s^{n/2}.$$

* For example (Current Paper 68[3]), the N.A.C.A. have published the formula of the NACA 0012 section in the form

$$\zeta = a_1 s^{1/2} + a_2 s + a_4 s^2 + a_6 s^3 + a_8 s^4$$

and the NACA 0012-63 section is given by a formula of the type

$$\left.\begin{aligned} \zeta_1 &= a_1 s^{1/2} + a_2 s + a_4 s^2 + a_6 s^3 \\ \zeta_2 &= b_0 + b_2 s + b_4 s^2 + b_6 s^3 \end{aligned}\right\}.$$

Again, the thickness distribution of the Clark Y section has been fitted to equations of the type

$$\left.\begin{aligned} \zeta_1 &= a_1 s + a_3 s^{3/2} + a_5 s^{5/2} + a_7 s^{7/2} \\ \zeta_2 &= b_0 + b_2 s + b_4 s^2 + b_6 s^3 + b_8 s^4 \end{aligned}\right\}.$$

In particular $a_0 = 0$, and it is usually sufficient to assume that $b_1 = b_3 = \ldots = b_{2m-1} = 0$, (*i.e.*, the rear part of the section may be fitted by a polynomial in s).

If the formula is made up of two different expressions (*i.e.*, $s_0 \neq 1$), the expression for I is lengthy and its calculation labourous. However, it may be shown that, if $s_0 = 1$, the expression for I reduces simply to

$$I = \sum_{p=1}^{2m} \sum_{q=1}^{2m} a_p a_q \left(\frac{2p}{p+q}\right) \left\{ \left[\frac{(-1)^q - (-1)^p}{2}\right] \ln 2 + \sum_{\nu=0}^{[(q-1)/2]} \frac{1}{q - 2\nu} - \sum_{\nu=0}^{[(p-3)/2]} \frac{1}{p - 2\nu - 2} \right\} \qquad (24)$$

the square brackets denoting the integral part of the upper limits of summation.

In particular, if the p's and q's are all even or all odd,

$$I = 2 \sum_{p=1}^{2m} \sum_{q=1}^{p-2} a_p a_q \left[\frac{1}{p} - \frac{p-q}{p+q}\left(\frac{1}{p-2} + \frac{1}{p-4} + \cdots + \frac{1}{q+2}\right)\right] + \sum_{p=1}^{2m} \left(\frac{a_p{}^2}{p}\right) \qquad (25)$$

We may apply equation (24) to the calculation of I for the N.A.C.A. uncambered 'four-figure' airfoil series, whose profiles are given by the formula :—

$$\tfrac{1}{2}\zeta = 1{\cdot}484 s^{1/2} - 0{\cdot}630 s - 1{\cdot}758 s^2 + 1{\cdot}421 s^3 - 0{\cdot}508 s^4.$$

These sections have a small finite thickness at the trailing edge, but as this is only 1 per cent of the maximum thickness its effect may be neglected. The nose radius of curvature of these sections is $1{\cdot}1 t^2/c$, the trailing-edge angle is $2{\cdot}3 t/c$ radians, and the maximum thickness is at 30 per cent chord. The value of I computed from equation (24) is $4{\cdot}47$.

4. *Effect of Changes of Profile Shape on Drag.*—4.1. *Effects of Changes in Nose Radius and Trailing-Edge Angle.*—Ideally, it would be useful to be able to state the drag of a wing section in terms of its main geometrical features ; for example, the nose radius of curvature, the chord-wise position of the maximum thickness, and the trailing-edge angle.

From the few worked examples of the last sections it will be noticed that sections which have a small radius of curvature and a small trailing-edge angle also tend to have a small drag. In general if a family of sections is described by an equation whose parameters are related to the three geometrical features named above, then this effect is very pronounced.

A simple example will illustrate this : if we choose as the family of profiles those given by the formula

$$\zeta(s) = \sum_{n=1}^{4} \beta_n \sin n\theta + B \sin^2\theta, \qquad \left(s = \frac{1 - \cos\theta}{2}\right)$$

the value of I is simply

$$I = \frac{\pi^2}{2} \sum_{n=1}^{4} n\beta_n{}^2 + 8\pi B\left(\frac{\beta_1}{3} - \frac{\beta_3}{5}\right) + 4B^2.$$

Accordingly the drag may be quoted in terms of :—

(*a*) leading-edge radius of curvature

(*b*) maximum thickness position, and

(*c*) trailing-edge angle

since the five parameters may be found in terms of these quantities, and the implied conditions that

(*d*) the section ordinate is known ($\zeta = 1$) at the chordwise position of maximum thickness

(*e*) the trailing-edge is sharp.

The results are shown in Fig. 6 where the value of $(I/4)$—which is the drag of the section relative to that of the biconvex profile—is plotted as a function of nose radius for various trailing-edge angles and positions of maximum thickness.

The increase in drag with increase in nose radius and trailing-edge angle is evident from an examination of the figures. But this effect has little significance either quantitatively or qualitatively. For we shall seek to show in the two following sections that :—

(i) an increase in trailing-edge angle leads to a *decrease* in drag (and under certain conditions so also does an increase in nose radius), if the necessary increase in the section ordinates only affects the shape of the profile over a limited and localised region of the chord (section 4.2) ;

(ii) a change in profile shape leaving the three named geometrical features *unaltered*, can produce a change in the drag of the same order as the difference in drag we are attempting to find (*i.e.*, the difference in drag between the chosen profile and that of the biconvex section), as shown in section 4.3.

These conclusions mean that the value of nose radius or trailing-edge angle is no guide to the drag of the section *per se*. The effect on drag of an increase in nose radius or trailing-edge angle will depend upon the way in which this increase modifies the shape of the rest of the section : the modification can—and generally does—produce an increase in drag, but if performed in a certain particular manner it can have the opposite effect.

4.2. *Localised Variations of Shape.*—To obtain an insight into the effect of localised variations of profile shape, let us assume that we change a profile whose ordinates are given by $\zeta = \zeta(s)$ by adding an infinitesimal increment so that the shape is given by

$$\zeta = \zeta(s) + \delta(s).$$

Then from equation (12),

$$\left.\begin{aligned} \delta I = \delta I_1 + \delta I_2 = 2\int_0^1\int_0^1 \delta'(\sigma)\zeta'(s)\ln\left|\frac{1}{s-\sigma}\right| ds\, d\sigma \\ + \int_0^1\int_0^1 \delta'(\sigma)\,\delta'(s)\ln\left|\frac{1}{s-\sigma}\right| d\delta\, ds \end{aligned}\right\} \quad \ldots \quad \ldots \quad \ldots \quad (26)$$

which we may express, as in equation (15), in the form

$$\delta I = -2\pi\left(\frac{c}{t}\right)\int_0^1 \delta(\sigma)\left[\frac{\Delta p}{q}\right]_{\mathrm{inc}} d\sigma + O(\delta'^2) \quad \ldots \quad \ldots \quad \ldots \quad \ldots \quad (27)$$

where $[\Delta p/q]_{\mathrm{inc}}$ is the linearised incompressible pressure distribution over the undistorted profile.

For the general group of profiles defined by equation (23) the pressure distribution is given by Ref. 3. Near the leading edge of the wing :—

$$\frac{\Delta p}{q} = a_2 \ln \frac{1}{\sigma} + C_1 + O(\sigma^{1/2}). \qquad (28)$$

Similarly near the trailing edge :—

$$\frac{\Delta p}{q} = \zeta_2'(1) \ln |1 - \sigma| + C_2 + O(1 - \sigma) \qquad (29)$$

where the values of the constants C_1 and C_2 are determined by the general shape of the profile, and may be either positive or negative.

It follows from equation (29) that, since $\zeta_2'(1)$ is negative for sections with a finite trailing-edge angle, $[\Delta p/q]_{\text{inc}}$ is positive near the trailing edge, and therefore from (27) any small increase in the ordinates near the trailing edge will *reduce* the drag. A change in the ordinates near the leading edge might work one way or the other, as for a round-nose airfoil the coefficient a_2 in equation (28), which has no simple geometrical significance, could be either positive or negative.

4.3. *Variation of the Shape of the* RAE 101 *Section*.—We shall now attempt to justify the fact that the drag can be changed significantly by a change in profile shape which leaves the nose radius and trailing-edge angle unaltered. This conclusion may be justified most easily by an example.

Let us consider a variation of the profile shape of the RAE 101 section. The change in drag due to an increase in the ordinates of the section at $s = \sigma$ of amount $\delta(\sigma)$ is given by equation (26), where the linearised incompressible pressure distribution over the undistorted section is given by[2]

$$\left.\begin{aligned}\left[\frac{\Delta p}{q}\right]_{\text{inc}} &= -2\cdot957\left(\frac{t}{c}\right) \qquad &&\text{for } 0 \leqslant \sigma \leqslant 0\cdot3\\ &= (5\cdot707\sigma - 4\cdot669)\left(\frac{t}{c}\right), &&\text{for } 0\cdot3 \leqslant \sigma \leqslant 1.\end{aligned}\right\} \qquad (30)$$

A variation which will produce a first-order decrease in I is such that

$$\delta(s) \leqslant 0 \text{ for } s \leqslant 0\cdot8$$
$$\delta(s) \geqslant 0 \text{ for } s \geqslant 0\cdot8$$

since $[\Delta p/q]_{\text{inc}} = 0$ approximately at $0\cdot8c$. In particular we have

$$\delta(0) = \delta(1) = 0$$

and we shall assume further that the leading-edge radius of curvature and the position of maximum thickness are left unchanged. Such a modification aft of the maximum thickness, however, is liable to introduce a concave curvature which is undesirable. Accordingly we shall assume

$$\begin{aligned}\delta(s) &= -\varepsilon[s^2(0\cdot3 - s)]^{3/2}, \qquad && s \leqslant 0\cdot3\\ &= 0, && s \geqslant 0\cdot3.\end{aligned}$$

We then find from equation (26) that

$$\delta I = -0\cdot0111\varepsilon + 0\cdot0000421\varepsilon^2.$$

If we are to avoid any concave curvature on the nose, ε must be less than about 35, so that if we chose $\varepsilon = 30$ we are making a 'reasonable' modification and we obtain a reduction in drag given by $\delta I = -0\cdot30$ so that $I = 3\cdot89$ (*i.e.*, a 7 per cent reduction of the figure quoted in Table 2 for the undistorted RAE 101 profile, bringing it to a value less than that of a biconvex section). The required change in the section ordinates are listed in Table 3 ; the changed shape is shown in Fig. 7 together with the effect on the pressure distribution, which is small.

4.4. *Variations for the Shape of the Double-Wedge Section.*—We shall now seek to show that the double-wedge section is that which has least drag for a given thickness at half-chord, if regions of concave curvature and discontinuous concave changes in profile slope are precluded.

The linearised incompressible pressure distribution over a double-wedge wing with maximum thickness at half-chord is given by :—

$$\left[\frac{\Delta p}{q}\right]_{\text{inc}} = \frac{t/c}{\pi} \ln \left[\frac{(\frac{1}{2} - \sigma)^2}{\sigma(1 - \sigma)}\right] . \qquad (31)$$

If we are to obtain any first-order decrease in drag by a small variation of the section shape, it follows from equations (27) and (31) that it is sufficient to increase the thickness near the leading or trailing edges (where the pressure is high) and decrease the thickness near the maximum thickness (where pressure is low). But the thickness cannot anywhere be decreased if the position of maximum thickness is left unaltered, since the curvature must not be concave. Thus the wing ordinates may only be increased.

Suppose that the incremental addition to the wing ordinate at $\sigma = \frac{1}{2} \pm \frac{1}{2\sqrt{2}}$, where $\left[\frac{\Delta p}{q}\right]_{\text{inc}} = 0$, is $|\varepsilon| > 0$. Then

$$\int_{\frac{1}{2}-\frac{1}{2\sqrt{2}}}^{\frac{1}{2}} \delta(\sigma) \left[-\frac{\Delta p}{q}\right]_{\text{inc}} d\sigma \geqslant \int_{\frac{1}{2}-\frac{1}{2\sqrt{2}}}^{\frac{1}{2}} 2\sqrt{2}|\varepsilon|\left(\frac{1}{2} - \sigma\right)\left[-\frac{\Delta p}{q}\right]_{\text{inc}} d\sigma$$

and

$$\int_{0}^{\frac{1}{2}-\frac{1}{2\sqrt{2}}} \delta(\sigma) \left[+\frac{\Delta p}{q}\right]_{\text{inc}} d\sigma \leqslant \int_{0}^{\frac{1}{2}-\frac{1}{2\sqrt{2}}} 2\sqrt{2}|\varepsilon|\left(\frac{1}{2} - \sigma\right)\left[+\frac{\Delta p}{q}\right]_{\text{inc}} d\sigma$$

because of the restriction on surface curvature. Thus

$$\int_{0}^{1/2} \delta(\sigma)\left[\frac{\Delta p}{q}\right]_{\text{inc}} d\sigma \leqslant 2\sqrt{2}|\varepsilon| \int_{0}^{1/2} \left(\frac{1}{2} - \sigma\right)\left[\frac{\Delta p}{q}\right]_{\text{inc}} d\sigma = 0, \quad \text{from (31).}$$

By considerations of symmetry, it follows that, in equation (26)

$$\delta I_1 \geqslant 0$$

and since δI_2 is essentially positive

$$\delta I > 0.$$

Hence any change of section shape which leaves the maximum thickness and its chordwise position unaltered, and does not introduce concave curvature, increases the drag.

If the maximum thickness position is ahead of the half-chord point, then the double-wedge section is no longer the shape having least drag and some thickening of the wing ahead of the maximum thickness position reduces the drag.

5. *Conclusions.*—(*a*) The drag in supersonic flow of an infinite swept wing with edges swept behind the Mach lines, may be expressed as the product of two terms, one a function of Mach number and of sweepback, and the other depending only on the section shape. It follows that the relative drag of two wings of different section is independent of Mach number (*see* equation (11)).

(*b*) If the shape of the wing section is given by a formula which is

(i) a Fourier series,

(ii) a conformal transformation of a circle,

or (iii) a general algebraic polynomial,

the drag of various sections may be computed in terms of the parameters of the formulæ, as given in equations (14), (22) and (24).

(*c*) The drag of various sections is proportional to the integral along the chord of the product of the section ordinate and the local value of the excess pressure existing over the profile according to the linearised incompressible-flow theory (*see* equation (15)).

(*d*) A wing of elliptic section has the least drag for a given cross-sectional area. It is possible to construct a section which has a drag smaller than any given finite value if only the maximum thickness of the section is fixed. If concave curvature of the surface is inadmissible, the double-wedge wing yields the least drag for a given half-chord thickness.

(*e*) The drag of infinite swept wings with sections having round noses and sharp trailing-edges is generally between 0 and 15 per cent greater than that of wings with biconvex section. The following figures refer to the relative drag of sections having the same maximum thickness:—

Ellipse	1·23
NACA 0012 series	1·12
RAE 101	1·05
Biconvex	1·00
Double-wedge (max t/c at $c/2$)	0·69

(*f*) An increase in nose radius or trailing-edge angle of a section generally leads to an increased drag, but this largely depends upon the manner in which this change affects the shape of the rest of the profile.

(*g*) It is possible to deduce the change of shape required to reduce the drag of any particular section if its low-speed pressure distribution is given.

(*h*) The absolute drag of high aspect ratio constant-chord wings is higher than that of the infinite wing with the same sweepback and wing section, but the difference is due to a term which varies inversely as the square of the wing aspect ratio. Thus it is reasonable to suppose that the results quoted above are a guide to the drag of finite wings of moderate aspect ratio (*e.g.*, $A \tan \Lambda \geqslant 4$) at low supersonic speeds.

LIST OF SYMBOLS

a		Radius of circle in (η, ζ)-plane
a_n, b_n		Coefficients of polynominal in $s^{1/2}$ representing $\zeta(s)$
b		Semi-span of wing
c		Chord of wing (measured in free-stream direction)
h		Distance of centre of circle in (η, ζ)-plane along real axis from origin
m	$=$	$\cot \Lambda$
Δp		Difference between local and static air pressure

q	$=$	$\frac{1}{2}\rho U^2$
s	$=$	X/c
t		Thickness of wing
u		Component of air velocity parallel to the x-axis
w		Component of air velocity parallel to the z-axis
$\left.\begin{matrix} x \\ y \\ z \end{matrix}\right\}$		System of Cartesian co-ordinates, origin at wing apex, the point $(c, 0, 0)$ being the wing root trailing edge, and the wing being in the plane $z = 0$
$z\ (X)$		Value of z as a function of X on surface of wing section
A		Wing aspect ratio $(=2b/c)$
C_D	$=$	D/qS
D		Wing drag at zero lift
I	$=$	$\int_0^1\int_0^1 \zeta'(s)\ \zeta'(\sigma)\ \ln\left\lvert\frac{1}{s-\sigma}\right\rvert ds\ d\sigma = \left[\frac{\pi(1-\mu^2)^{3/2}}{(3-\mu^2)}\right]\frac{D}{qm^2t^2}$
$(I/4)$		Drag of section relative to that of biconvex section
M		Mach number of speed of wing relative to air
S		Wing area $(=2bc)$
U		Free-stream velocity
V		Cross-sectional area of wing section $\left(=\int_0^c z(X)\,dx\right)$
(dW/dY)	$=$	$u - iw$
X	$=$	$x - y/m$
Y	$=$	$x + iz$
$\mathscr{R}(\ )$		real part of ( )
$\mathscr{I}(\ )$		imaginary part of ( )
H	$=$	$\xi + i\eta$
H'	$=$	$H - h$
Λ		Angle of sweep of wing leading edge
α		Trailing-edge total angle
α_n		Coefficient of H^{-n} in conformal transformation between Y and H
$\alpha_n{}^*$		Real part of α_n
β_n		Coefficient of $\sin n\theta$ in Fourier series for $\zeta(s)$
$\delta(s)$		Incremental change in $\zeta(s)$
ε		Semi-angle of wedge (except in section 4.4)
$\zeta(s)$	$=$	$2z(X)/t$
$\zeta'(s)$	$=$	$d\zeta/ds$
(η, ζ)		System of co-ordinates in plane of flow about a circle
θ		$\text{arc cos}\ (1 - 2s)$
μ		$m\sqrt{(M^2 - 1)}$
ξ		Value of X corresponding to leading edge of source plane considered
ρ		Air density
ϱ		$\frac{\text{Leading-edge radius of curvature}}{\text{Wing chord}}$ in Fig. 6
σ	$=$	ξ/c
τ	$=$	Thickness/chord ratio
ψ		Half-depth of streamtube at $x = -\infty$
$F\vert_X$ etc.		Value of the function F with X (a variable) held as constant and arbitrary

REFERENCES

No.	Author	Title, etc.
1	R. T. Jones	Thin Oblique Airfoils at Supersonic Speed. N.A.C.A. Tech. Note 1107. 1946.
2	R. C. Pankhurst and H. B. Squire ..	Calculated Pressure Distributions for the RAE 100–104 Aerofoil Sections. R.A.E. Tech. Note Aero 2039. A.R.C. 13,254. 1950.
3	S. Goldstein	Approximate Two-dimensional Aerofoil Theory. Part I. Velocity Distributions for Symmetrical Aerofoils. Current Paper 68. June, 1942.
4	S. M. Harmon	Theoretical Supersonic Wave Drag of Untapered Sweptback and Rectangular Wings at Zero Lift. N.A.C.A. Tech. Note 1449. 1947.
5	R. T. Jones	Leading Edge Singularities in Thin Airfoil Theory. *J. Aero. Sci.*, Vol. 17, No. 5. May, 1950.
6	T. Nonweiler..	The Theoretical Wave Drag at Zero Lift of Fully Tapered Swept Wings of Arbitary Section. College of Aeronautics Rpt. 76. October, 1953. (To be published.)

TABLE 1

Relative Drag of Various Sections

Section	Formula	Maximum thickness position*	L.E.	T.E.	I
Ellipse	$\zeta(s) = 2[(1-s)s]^{1/2}$	$\frac{1}{2}c$	Round	Round	$\frac{\pi^2}{2} = 4 \cdot 93$
Conventional	$\zeta(s) = \frac{3\sqrt{3}}{2}(1-s)(s)^{1/2}$	$\frac{1}{3}c$	Round	Angular	$\frac{9}{2} = 4 \cdot 50$
Joukowski	$\zeta(s) = \frac{16}{3\sqrt{3}}(1-s)^{3/2}(s)^{1/2}$	$\frac{1}{4}c$	Round	Cusped	$\frac{4\pi^2}{9} = 4 \cdot 39$
Biconvex	$\zeta(s) = 4(1-s)s$	$\frac{1}{2}c$	Angular	Angular	$4 = 4 \cdot 00$
Biconvex cusped	$\zeta(s) = \frac{25}{6}\sqrt{\frac{5}{3}}(1-s)^{3/2}s$	$\frac{2}{5}c$	Angular	Cusped	$\frac{625}{162} = 3 \cdot 86$
Double-cusp	$\zeta(s) = 8[(1-s)s]^{3/2}$	$\frac{1}{2}c$	Cusped	Cusped	$\frac{3\pi^2}{8} = 3 \cdot 70$
Double-wedge	Discontinuous	$\frac{1}{2}c$	Angular	Angular	$4 \ln 2 = 2 \cdot 77$
,, ,,		$\frac{1}{3}c$			$\left(\frac{3}{2}\ln 3 + 3\ln\frac{3}{2}\right) = 2 \cdot 87$
,, ,,		$\frac{1}{4}c$			$\left(\frac{4}{3}\ln 4 + 4\ln\frac{4}{3}\right) = 2 \cdot 99$
Flat-sided Double-wedge	Discontinuous	$0 \cdot 15c$ to $0 \cdot 45c$	Angular	Angular	$4 \cdot 56$

* The drag is unaltered when the sections are reversed (*i.e.*, when s is changed to $-s$). It is assumed that profiles with the maximum thickness behind the half-chord are of little interest.

TABLE 2

Drag of RAE 100–104 *Sections*

Section	Maximum t/c position per cent chord	$\frac{\text{L.E. radius} \times \text{chord}}{(\text{thickness})^2}$	$\frac{\text{T.E. angle (radn)}}{(t/c)}$	I
RAE 100	27·0	1·10	1·71	4·38
101	31·0	0·76	1·79	4·19
102	35·6	0·69	1·91	4·21
103	39·0	0·63	2·09	4·31
104	41·9	0·59	2·37	4·42

TABLE 3

Modification to Nose Shape of RAE 101 *Section to Effect* 7 *per cent Reduction in Drag*

s	Ordinates of unmodified section (Maximum thickness = 2)	Ordinates of modified section (Maximum thickness = 2)
0	0	0
0·005	0·1741	0·1723
0·01	0·2453	0·2406
0·025	0·3834	0·3663
0·05	0·5319	0·4901
0·1	0·7215	0·6368
0·15	0·8440	0·7428
0·2	0·9261	0·8414
0·25	0·9770	0·9351
0·3	0·9994	0·9994

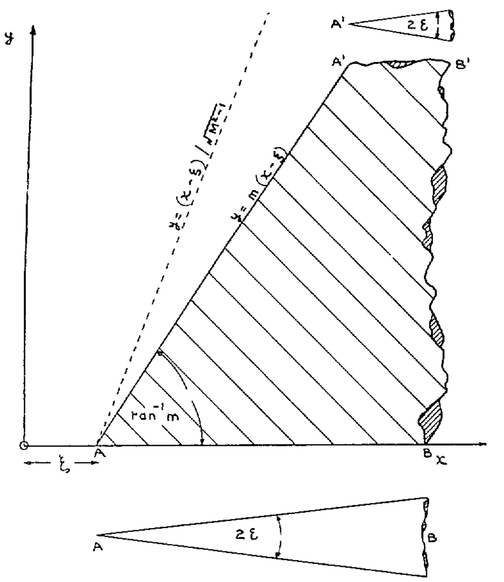

FIG. 1. Source plane of strength ε bounded by lines $y = m(x - z)$ and $y = 0$.

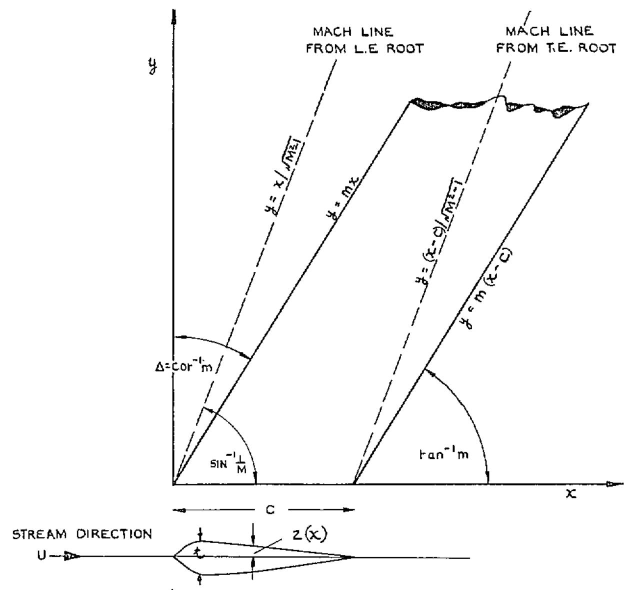

FIG. 2. Symbols for swept wings.

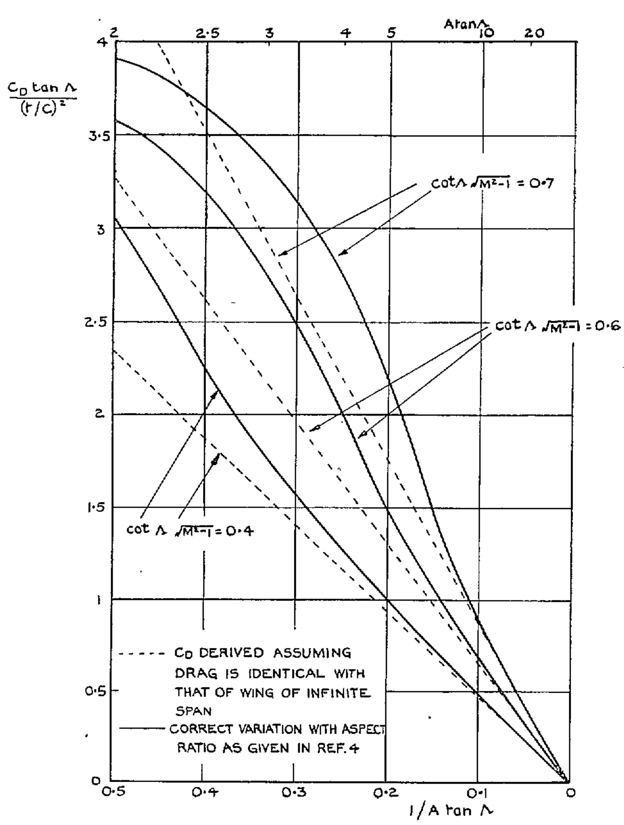

FIG. 3. Variation of drag with span of wings with biconvex section.

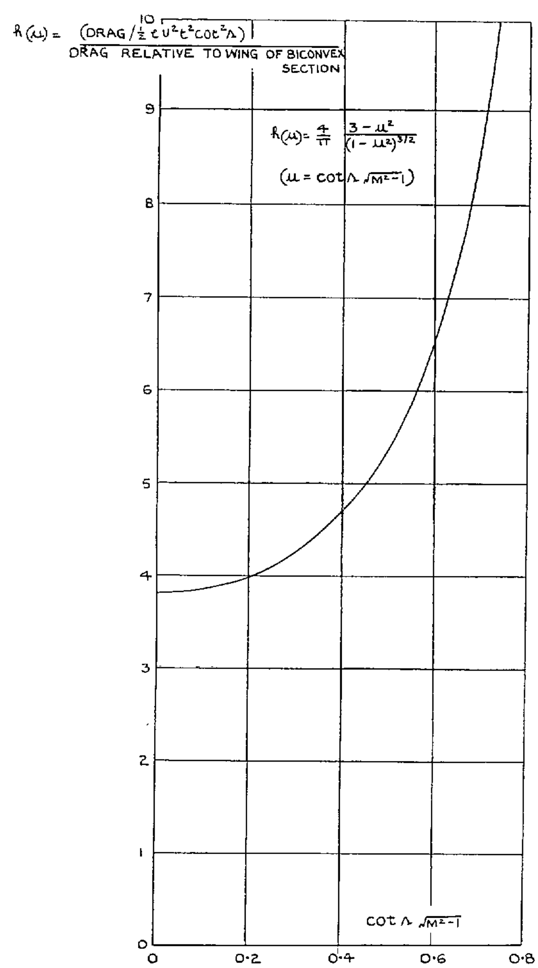

FIG. 4. Variation of drag of infinite swept wing with arbitrary section as a function of Mach number.

B

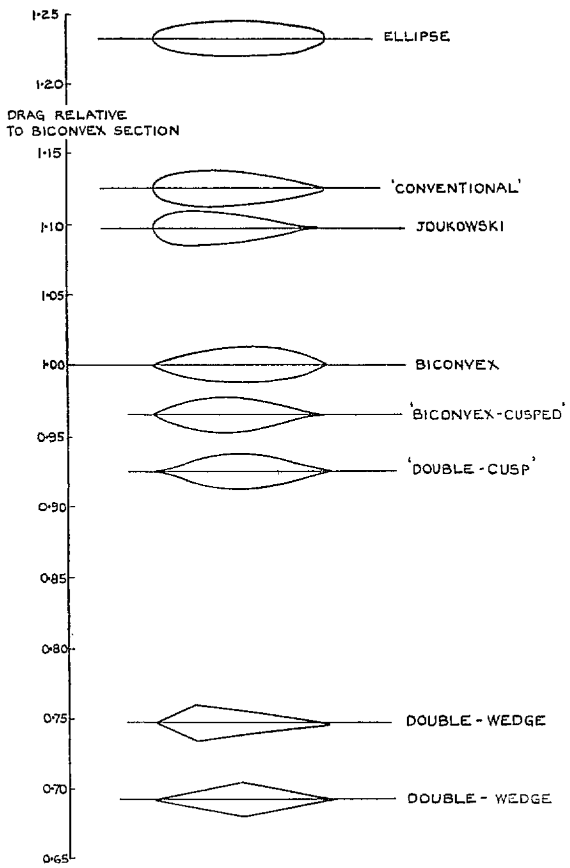

FIG. 5. Relative drags of infinite swept wings with various sections of the same thickness.

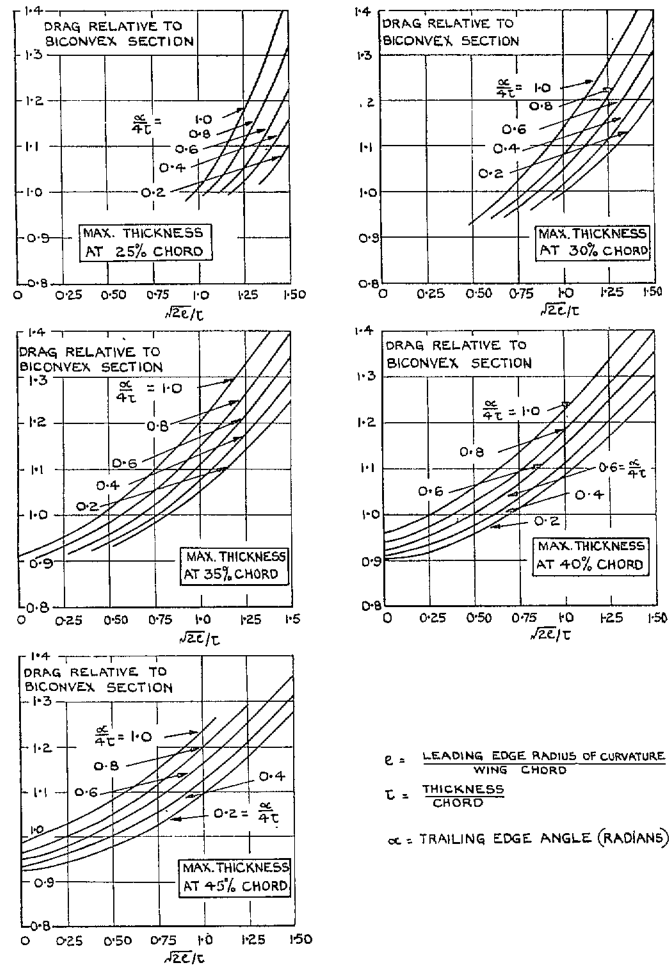

FIG. 6. Effect of leading-edge curvature and trailing-edge angle on drag of a family of wings.

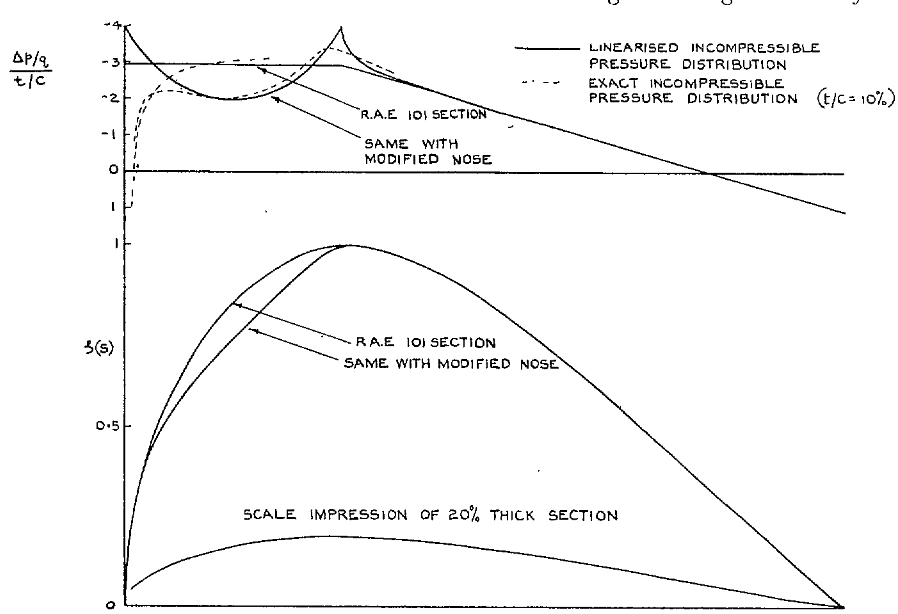

FIG. 7. Effect of modification to nose shape of RAE 101 section whereby drag is reduced by 7 per cent.

J4293 Wt. 17/680 K9 11/54 D&Co. 34/263

PRINTED IN GREAT BRITAIN

Publications of the Aeronautical Research Council

ANNUAL TECHNICAL REPORTS OF THE AERONAUTICAL RESEARCH COUNCIL (BOUND VOLUMES)

1936 Vol. I. Aerodynamics General, Performance, Airscrews, Flutter and Spinning. 40s. (41s. 1d).
Vol. II. Stability and Control, Structures, Seaplanes, Engines, etc. 50s. (51s. 1d.)
1937 Vol. I. Aerodynamics General, Performance, Airscrews, Flutter and Spinning. 40s. (41s. 1d.)
Vol. II. Stability and Control, Structures, Seaplanes, Engines, etc. 60s. (61s. 1d.)
1938 Vol. I. Aerodynamics General, Performance, Airscrews. 50s. (51s. 1d.)
Vol. II. Stability and Control, Flutter, Structures, Seaplanes, Wind Tunnels, Materials. 30s. (31s. 1d.)
1939 Vol. I. Aerodynamics General, Performance, Airscrews, Engines. 50s. (51s. 1d.)
Vol. II. Stability and Control, Flutter and Vibration, Instruments, Structures, Seaplanes, etc. 63s. (64s. 2d.)
1940 Aero and Hydrodynamics, Aerofoils, Airscrews, Engines, Flutter, Icing, Stability and Control, Structures, and a miscellaneous section. 50s. (51s. 1d.)
1941 Aero and Hydrodynamics, Aerofoils, Airscrews, Engines, Flutter, Stability and Control, Structures. 63s. (64s. 2d.)
1942 Vol. I. Aero and Hydrodynamics, Aerofoils, Airscrews, Engines. 75s. (76s. 3d.)
Vol. II. Noise, Parachutes, Stability and Control, Structures, Vibration, Wind Tunnels. 47s. 6d. (48s. 7d.)
1943 Vol. I. Aerodynamics, Aerofoils, Airscrews, 80s. (81s. 4d.)
Vol. II. Engines, Flutter, Materials, Parachutes, Performance, Stability and Control, Structures. 90s. (91s. 6d.)
1944 Vol. I. Aero and Hydrodynamics, Aerofoils, Aircraft, Airscrews, Controls. 84s. (85s. 8d.)
Vol. II. Flutter and Vibration, Materials, Miscellaneous, Navigation, Parachutes, Performance, Plates, and Panels, Stability, Structures, Test Equipment, Wind Tunnels. 84s. (85s. 8d.)

ANNUAL REPORTS OF THE AERONAUTICAL RESEARCH COUNCIL—

1933–34	1s. 6d. (1s. 8d.)	1937	2s. (2s. 2d.)
1934–35	1s. 6d. (1s. 8d.)	1938	1s. 6d. (1s. 8d.)
April 1, 1935 to Dec. 31, 1936.	4s. (4s. 4d.)	1939–48	3s. (3s. 2d.)

INDEX TO ALL REPORTS AND MEMORANDA PUBLISHED IN THE ANNUAL TECHNICAL REPORTS, AND SEPARATELY—

April, 1950 - - - - - R. & M. No. 2600. 2s. 6d. (2s. 7½d.)

AUTHOR INDEX TO ALL REPORTS AND MEMORANDA OF THE AERONAUTICAL RESEARCH COUNCIL—

1909–1949 - - - - - - R. & M. No. 2570. 15s. (15s. 3d.)

INDEXES TO THE TECHNICAL REPORTS OF THE AERONAUTICAL RESEARCH COUNCIL—

December 1, 1936 — June 30, 1939.	R. & M. No. 1850.	1s. 3d. (1s. 4½d.)
July 1, 1939 — June 30, 1945.	R. & M. No. 1950.	1s. (1s. 1½d.)
July 1, 1945 — June 30, 1946.	R. & M. No. 2050.	1s. (1s. 1½d.)
July 1, 1946 — December 31, 1946.	R. & M. No. 2150.	1s. 3d. (1s. 4½d.)
January 1, 1947 — June 30, 1947.	R. & M. No. 2250.	1s. 3d. (1s. 4½d.)
July, 1951 - - - - -	R. & M. No. 2350.	1s. 9d. (1s. 10½d.)

Prices in brackets include postage.

Obtainable from

HER MAJESTY'S STATIONERY OFFICE

York House, Kingsway, London W.C.2 ; 423 Oxford Street, London W.1 (Post Orders : P.O. Box No. 569, London S.E.1) ; 13A Castle Street, Edinburgh 2 ; 39 King Street, Manchester 2 ; 2 Edmund Street, Birmingham 3 ; 1 St. Andrew's Crescent, Cardiff ; Tower Lane, Bristol 1 ; 80 Chichester Street, Belfast OR THROUGH ANY BOOKSELLER

S.O. Code No. 23-2795